JP1.4 OBSERVATIONS AND INFLUENCE OF GROUNDWATER ON SURFACE FLUXES USING THE NOAH LAND SURFACE MODEL IN THE NEBRASKA SAND HILLS

David B. Radell* and Clinton M. Rowe
Department of Geosciences, University of Nebraska-Lincoln, Lincoln, NE, USA

1. INTRODUCTION

The Nebraska Sand Hills (Fig. 1) are a unique part of the Missouri River Basin that can be expected to exert an influence on the local and regional atmosphere due to their size and unique physiological characteristics. The Sand Hills are characterized by approximately 50,000 km^2 of rolling sand sheets and dunes, with a typical elevation of 1 km above sea level and local relief of the highest dunes near 0.1 km (Bleed and Flowerday 1998). Most of the region is covered with short rangeland grass and shrub vegetation, although inter-dune wetland areas consisting of denser mixtures of short prairie grasses occupy an estimated 4000 km^2 (Gosselin *et al.* 2006). The inter-dune regions are unique, in that the water table can vary significantly with the seasons and it is often close to the land surface, contributing additional water vapor to local evapotranspiration (ET). From an atmospheric perspective, this region is a unique location to observe and document the physical interactions that occur between the land surface and the atmosphere.

2. MODEL SETUP AND DESCRIPTION

Data from three Energy Budget-Bowen Ratio (EBBR) meteorological observing towers were used in this study to examine the exchange of heat and moisture from the land surface. The EBBR towers are located near Gudmundsen, NE in the northwestern region of the state (Fig. 1), at the University of Nebraska's Gudmundsen Sand Hills Research Laboratory (GSL). The meteorological sites are bounded within an approximate 6 km^2 area and sample a wet inter-dune ("wet valley") site, a dry inter-dune site ("dry valley") and dunal upland site ("updune"). The proximity of the sites (Fig. 1) permit a detailed look at their respective influence on the atmospheric environment, as each contains different soil and vegetative characteristics. The wet valley site lies in a sub-irrigated meadow and contains a dense canopy of vegetation. The dry valley site contains a sparser vegetation canopy than the wet valley, while the updune location has the sparsest vegetation and resides 10-15 m above the valley sites. Chen and Hu (2004) report that the mean monthly depth to subsurface water at the Gudmundsen wet valley varies throughout the year (Fig. 2). As ET in the Sand Hills exceeds precipitation throughout much of the annual cycle (507 mm to 358 mm at the wet valley in 2004), the influence of groundwater on the root zone and entire soil moisture profile in this region is vitally important.

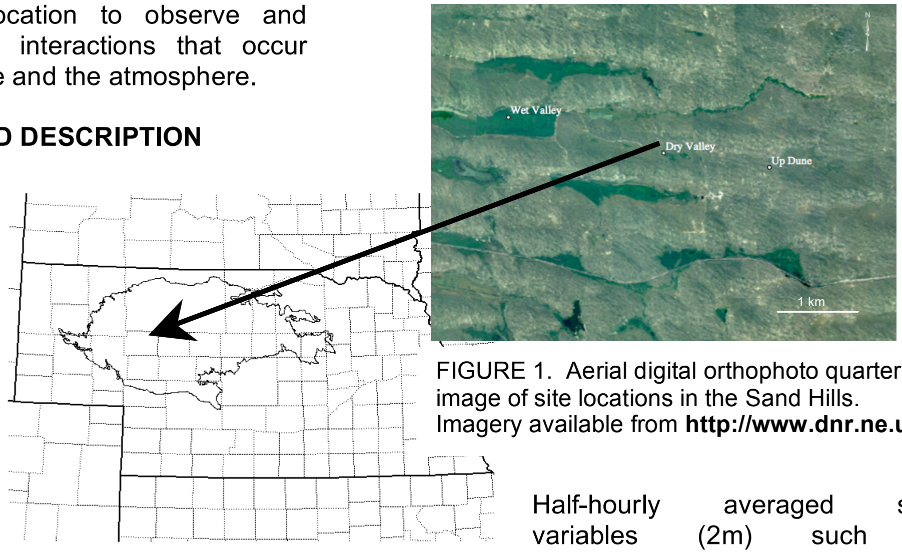

FIGURE 1. Aerial digital orthophoto quarter quad image of site locations in the Sand Hills. Imagery available from **http://www.dnr.ne.us**

Half-hourly averaged state variables (2m) such as temperature, relative humidity, incoming solar radiation, and surface pressure from the EBBR towers were used to drive the National Centers for Environmental Prediction, Oregon State University, Air Force Weather Agency, Hydrological Research Lab--Land Surface Model (NOAH-LSM) to test its ability to capture the annual and diurnal surface fluxes in the Sand Hills. A detailed description of the NOAH-LSM is available from Chen and Dudhia

---

Corresponding author address: D.B. Radell, Meteorology/Climatology Program, 214 Bessey Hall, University of Nebraska-Lincoln, Lincoln, NE, 68588. *email: dradell@papagayo.unl.edu*

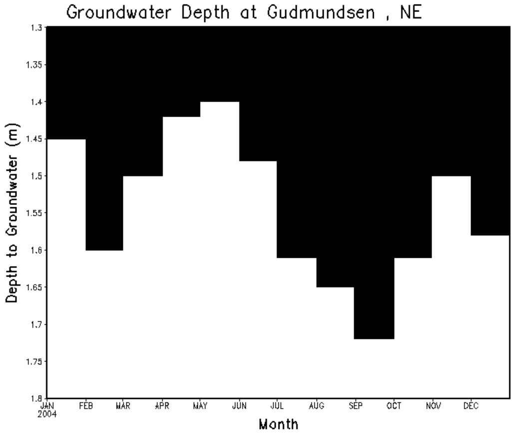

FIGURE 2. Observed mean monthly depth (m) to subsurface water at the wet valley.

(2001) and Sridhar *et al.* (2002). The NOAH-LSM was chosen for this study due to its success in regions of semiarid climate similar to those of the Sand Hills, such as the Konza Prairie in Kansas (Chen *et al.* 1996) and the Upper San Pedro River Basin in southeastern Arizona (Hogue *et al.* 2005). The NOAH-LSM is also coupled to many operational and research weather forecasting models, owing to its success in capturing the diurnal and annual cycles of surface fluxes.

Parameter estimations for the initial and boundary conditions used in the NOAH-LSM model runs were achieved through a variety of methods for the soil and vegetative properties. Soil parameters were largely based on available local field data or estimated through the empirically-derived data of Cosby *et al.* (1984). Vegetation parameters were based on the values for the "groundcover" classification of Chen and Dudhia (2001). Vegetation fractional coverage was estimated via available high resolution NDVI data and converted to a fractional coverage.

One major limitation of employing the uncoupled NOAH-LSM in the Sand Hills is the absence of a source of groundwater from below into the lowest model soil layer. Subsurface groundwater is an important component of the Sand Hills water cycle--in an area where ET exceeds precipitation throughout much of the year--and a crucial entity in providing a reasonable soil moisture profile. Within the root zone, defined in this study as the first 100 cm of soil, proper representation of soil water is necessary for the correct computation of ET and ultimately the proper partitioning of the surface energy fluxes.

Adjustments to account for the influence of the varying water table on the local energy budget were made for the wet and dry valley locations (Fig. 2). For each site, to account for the varying depth of the water table on a monthly basis, the data of Chen and Hu (2004) were used (see their Figure 7). These data were established for the wet valley location, and as they are the only such robust depth to subsurface water data available over a "climatological" time frame, they are assumed reasonable values for both sites. In order to compute the monthly soil water content of the fourth model soil layer, the depth to the water table was weighted based on its location within the lowest 2 m of soil. In short, a linear weighting function was implemented and can be written as,

$$W = \frac{z_{mon} - |z_{i=4}|}{|z_{i=3} - z_{i=4}|} \qquad \textbf{(1)}$$

where z is the depth of the i^{th} soil layer and z_{mon} is the depth to the water table for the given month (Fig. 2). The soil moisture content for the lowest soil layer ($S_{i=4}$) is then given by **(2)**, where S_{max} is

$$S_{i=4} = \begin{cases} [(S_{\max} \times W) + ((1 - W) \times S_{ref})], & z_{\text{mon}} \geq z_{i=4} \\ S_{i=4} & \text{otherwise} \end{cases} \qquad \textbf{(2)}$$

the value of the soil moisture at saturation and S_{ref} the soil moisture at field capacity. Thus, the closer the water table to the surface, the more weight given to the soil water content in the lowest layer by the saturated soil water content value. The deeper the water table, the more weight given by the unsaturated soil water content. For example, in the month of January, the observed depth of the water table was 1.45 m and in February it was 1.60 m. Therefore, the soil water value in the fourth model layer will be weighted closer to soil saturation in January than in February.

3. RESULTS

Comparisons were made for each site between observations and the model simulations with ("groundwater" or "gw" experiment) and without ("control" or "ctl" experiment) groundwater influence. No observations were available for the wet valley location and so no opportunity existed to compare the model results after the adjusted depth of the water table for soil moisture. For the dry valley location, however, soil moisture values

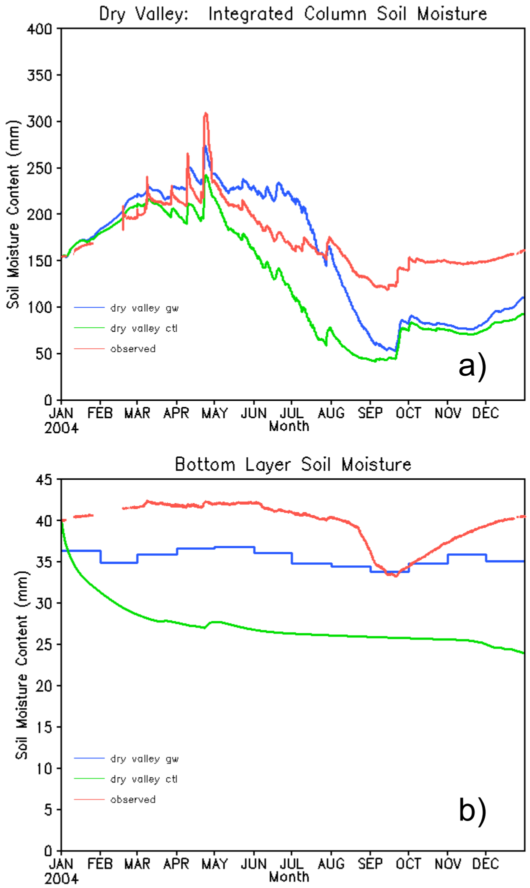

FIGURE 3. Annual volumetric soil moisture (mm) in the (a) top three and (b) lowest model layer for the dry valley.

were available and compared to the NOAH-LSM model runs (Fig. 3). The influence of the monthly varying depth to subsurface water ("gw" in Fig. 3) is seen to have an immediate effect on the total column soil water. From January to August 2004, the NOAH-LSM run with groundwater influence tended to better estimate the actual soil moisture in the top three model soil points (Fig. 3a). There were instances of soil moisture overestimation with individual precipitation events in February and March, and by April there is a consistent excess of about 25 mm of soil moisture relative to the control experiment (ctl). As evapotranspiration and surface runoff are the only sinks to incident precipitation due to the additional water from below in the groundwater experiment, it is likely that additional time was required to remove the increased soil moisture as compared to the control experiment. By late summer, ET is sufficient to deplete even the excess soil moisture provided by the subsurface water contribution. In the lowest soil level, soil moisture is better represented by the addition of the subsurface water, as near saturated values are observed throughout the entire annual cycle (Fig. 3b) at the dry valley.

The largest influence of the water table on ET occurs during the warm season (June-September), with potential ET at a maximum this time of year (Gosselin *et al.* 2006) and a slower depletion of total column soil water when groundwater is considered, compared to the control model run. The difference in the model soil moisture profile at each location due to the addition of the groundwater source affects the diurnal and annual surface fluxes. While still overestimated at the wet valley, sensible heat fluxes over the diurnal cycle (Fig. 4a) are improved, particularly during the afternoon. Peak values, near 1330 local time (LT), are improved by 40-50 W m^{-2}. Moreover, the transitional periods between 0600-0900 LT and 1800-2100 LT with

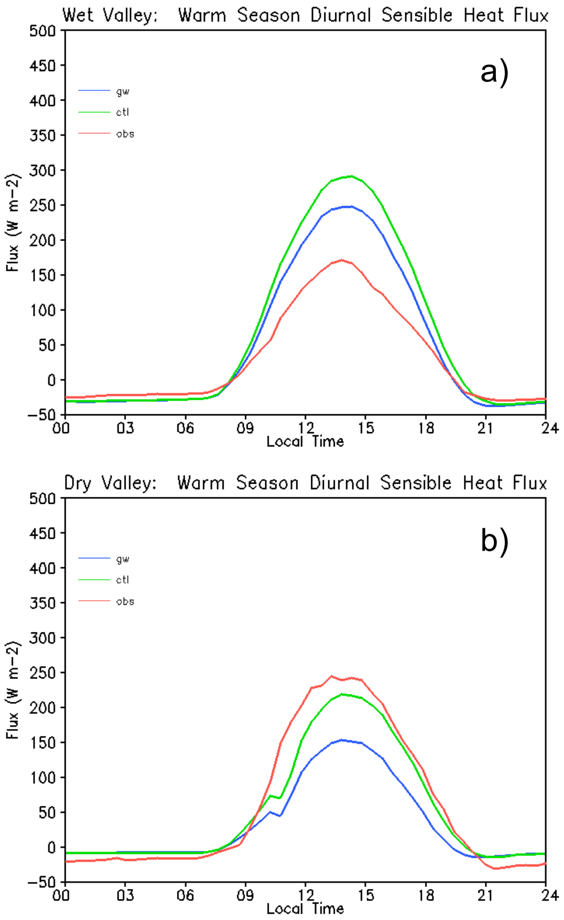

FIGURE 4. Diurnal mean sensible heat flux (W m^{-2}) for the (a) wet and (b) dry valley

groundwater influence are closer to the observed sensible heat flux. With a typically wetter soil column in the groundwater experiment relative to the control experiment, more energy went into latent heating at this location (not shown). At the dry valley (Fig. 4b), the increased surface soil moisture in the groundwater experiment tended to underestimate (overestimate) the sensible (latent) heat flux.

Examination of the ET with and without the influence of subsurface water provides insight into the annual effects (Table 1). The annual observed ET at the wet valley is more than twice that of the dry valley, at 582.6 and 276.1 mm, respectively. Even with a better estimation of soil moisture at the lowest model level, the NOAH-LSM tended to overestimate the annual ET at the dry valley, both with and without the addition of groundwater. This suggests that the upward diffusion of soil water in the dry valley model simulation is too quick (Fig. 3), particularly during late summer when ET is overestimated while soil moisture is underestimated (Fig. 3). The simulation of ET at the wet valley site is vastly improved with the influence of subsurface water. A net overestimation of only 3.5 mm of annual ET and a difference of only 0.01 mm of mean daily ET exhibit the effectiveness of the addition of the monthly-variant depth to subsurface water.

	Total ET (mm)	**Mean Daily ET (mm)**
DRY OBS	276.1	0.75
DRY GW	579.4	1.58
DRY CTL	437.3	1.19
WET OBS	582.6	1.60
WET GW	586.1	1.61
WET CTL	426.5	1.24

Table 1. Annual observed and modeled cumulative and mean daily ET (mm) for the wet and dry valley locations.

4. SUMMARY

The NOAH-LSM was modified to include the influence of subsurface water at two inter-dune regions in the Nebraska Sand Hills where the water table is near the surface. Mean monthly depths to subsurface water were used with a weighting function to adjust the soil moisture at the lowest model soil level. The effect of this additional soil water on ET and the surface fluxes were examined. The NOAH-LSM overestimated the annual ET and latent heat flux while underestimated the sensible heat flux at the dry valley site, where the groundwater is likey less an influence on the upper soil moisture. At the wet valley site, the addition of subsurface water improved the diurnal and annual estimation of ET. This in turn improved the partitioning of the latent and sensible heat fluxes to better represent the observed values. In the absense of a more sophisticated hydrologic model coupled to the NOAH-LSM, this simple yet effective method of accounting for the influence of subsurface water on soil moisture can be used with good accuracy if reliable data on depth to subsurface water are available.

5. ACKNOWLEDGEMENTS

This project was part of the Sand Hills Biocomplexity Project supported by the National Science Foundation (BE03-22076). We thank the Research Computing Facility at the University of Nebraska-Lincoln for use of their supercomputers, as well as K. Hubbard and R. Oglesby for their insightful comments and suggestions.

6. REFERENCES

Bleed, A., and C. Flowerday, (Eds.), *An Atlas of the Sand Hills*, Resource Atlas, No. 5a, Conservation and Survey Division, University of Nebraska, Lincoln, NE, pp. 67–92.

Chen, F. and J. Dudhia, 2001: Coupling of an advanced land surface-hydrology with the Penn State-NCAR MM5 modeling system. Part I: Model implementation and sensitivity. *Mon. Wea. Rev.,* **129**, 569-585.

Chen, F, K. Mitchell, J. Schaake, Y. Xue, H.-L. Pan, V. Koren, Q. Duan, M. Ek and A. Betts, 1996: Modeling of land surface evaporation by four schemes and comparison with FIFE observations. *J. Geosphys. Res*., **101(D3)**, 7251-7266.

Chen, X., and Q. Hu, 2004: Groundwater influences on soil moisture and surface evaporation. *J. Hydrol.,* **297**, 285-300.

Cosby, B. J., G. M. Hornberger, R .B. Clapp, and T. R. Ginn, 1984: A statistical exploration of the relationships of soil moisture characteristics to the physical properties of soils. *Water Resour*. *Res*., **20**, 682-690.

Gosselin, D. C., V. Sridhar, F. E. Harvey, and J. Goeke, 2006: Hydrological effects and groundwater fluctuations in interdunal environments in the Nebraska Sandhills. *Gr. Plains. Res.*, **16**, 17-28.

Hogue, T. S., L. Bastidas, H. Gupta, S. Sorooshian, K. Mitchell and W. Emmerich, 2005: Evaluation and transferability of the Noah land surface model in semiarid environments. *J. Hydrometeor*., **6**, 68-84.

Sridhar, V. and R. L. Elliott, F. Chen, and J. A. Brotzge 2002: Validation of the NOAH-OSU land surface model using surface flux measurements in Oklahoma. *J. Geophys. Res.,* **107**(D20), 4418, doi:10.1029/2001JD001306.